

## Frequency encoding by Bloch-Siebert shift

Zhipeng Cao<sup>1,2</sup>, Eduard Y. Chekmenev<sup>1</sup>, and William A. Grissom<sup>1,2</sup>

<sup>1</sup>Institute of Imaging Science, Vanderbilt University, Nashville, TN, United States, <sup>2</sup>Biomedical Engineering, Vanderbilt University, Nashville, TN, United States

**Target Audience:** MR engineering researchers interested in alternative spatial encoding mechanisms.

**Introduction:** Conventional MR imaging uses linear  $B_0$  gradients for spatial encoding. However,  $B_0$  gradients have high cost and bulk, and lead to patient discomfort via acoustic noise and peripheral nerve stimulation. A few spatial encoding methods have been proposed that use only RF gradient coils [1-4], which would not suffer the drawbacks of  $B_0$  gradients. However, existing RF gradient encoding methods severely restrict the types of sequences and subsequently image contrast that can be obtained. What is needed is an RF encoding method that leads to the same orthogonality between spatial encoding and image contrast that is enjoyed by conventional  $B_0$  gradients. Recently, promising results have demonstrated that RF encoding using the Bloch-Siebert (BS) shift could meet this need [5]. However, that work addressed only BS phase encoding, wherein an off-resonant pulse is used to generate a phase shift prior to signal acquisition, to acquire signal from a single k-space location. We present a theoretical description and simulation results demonstrating how the BS shift can be used for frequency encoding, wherein an off-resonant pulse is played out simultaneously with signal acquisition, to enable faster scanning via simultaneous k-space traversal and signal acquisition.

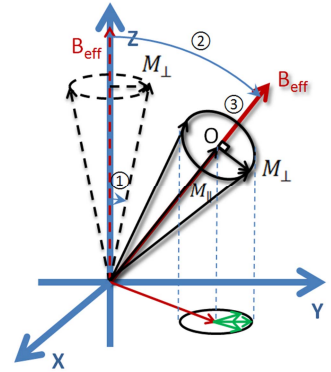


**Figure 1.** Vector depiction of BS frequency encoding in the frame rotating at  $\omega + \omega_{RF}$ .

**BS Frequency Encoding Theory:** 1) Sequence. The proposed BS frequency encoding sequence comprises three major intervals (Figs. 1 and 2). After longitudinal magnetization is excited to produce transverse magnetization  $M_{\perp}$  (interval 1), an adiabatic sweep [6] is applied using an RF gradient coil to rotate the cone of excited magnetization towards the transverse plane (interval 2), where it is kept locked during simultaneous data acquisition at Larmor frequency  $\omega_0$  and RF frequency encoding at frequency  $\omega_0 + \omega_{RF}$  (interval 3). The corresponding RF pulse sequence diagram is shown in Fig. 2. Interval 3a is the pre-phasing process, while the signal acquisition occurs at interval 3b. 2) Signal Equation. A signal expression can be derived based on trigonometric relationships. The locked magnetization  $M_{\perp}$  traces an elliptical path in the transverse XY plane. The detectable MR signal of each voxel at Larmor frequency  $\omega_0$  can be derived as  $S(t) \propto \exp(i\omega_{RF}t) \int dx \{ |M_{\perp}(x)| (\cos(\phi_{init}(x) - \phi(x, t)) + i \sin(\phi_{init}(x) - \phi(x, t)) \cos(\Psi(x))) \}$  (Eq. 1). Here,  $\phi_{init}$  is the initial phase of  $M_{\perp}$  before the encoding, and  $\Psi$  is the angle between the plane perpendicular to  $B_{eff}$  and the X-Y plane during interval 3b,  $\phi(x, t) = 2\pi k(t) \cdot x = \frac{\gamma}{2\pi} \int_0^t dt' \frac{\partial B_{eff}(x, t')}{\partial x} \cdot x$ ,  $B_{eff}(x, t) = \sqrt{|B_1^+(x, t)|^2 + \left(\frac{\omega_{RF}(t)}{\gamma}\right)^2}$ . (Note, with conventional  $B_0$  gradient encoding,  $\omega_{RF} = 0$ ,  $\cos(\Psi) = 1$ ,  $\phi(x, t) = 2\pi k(t) \cdot x = \gamma \int_0^t dt' G(x, t') \cdot x$ ) 3) Image Reconstruction. Because the signal precesses elliptically due to the  $\cos(\Psi)$  term, the detected signal has a non-linear dependence on the complex transverse magnetization  $M_{\perp}$ . Thus image reconstruction must comprise a fit of  $|M_{\perp}|$ , and  $\phi_{init}$  at each spatial location to the nonlinear signal model. 4) Acquired Resolution. Assuming a linear RF field gradient  $B_1(x) = cx$ , for a given desired spatial resolution  $\Delta x$  and  $\omega_{RF}$ , the required total sampling duration  $T$  is dictated by the spatial location in the object with the lowest  $|B_1^+|$  amplitude, according to  $T = \frac{\omega_{RF}}{\gamma^2 c^2 x \Delta x}$ .

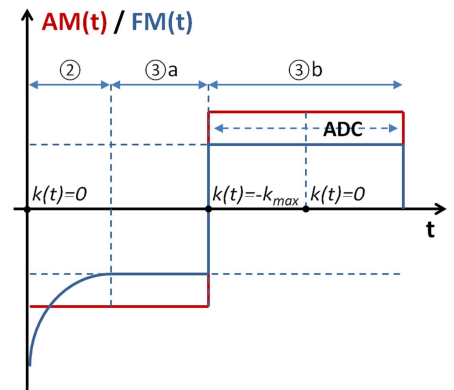


**Figure 2.** Pulse sequence depiction of AM and FM RF waveforms for BS frequency encoding.

**Methods:** To validate the proposed sequence design, signal expression, and reconstruction, a simulation study was performed in MATLAB. A 1D magnetization profile with a linear  $|B_{BS}|$  field was used to simulate the signal evolution (intervals 2&3) shown in Figs. 1 and 2. The 1D object was 5 mm in resolution and 100 mm in size, with 60 degree flip angle homogeneous excitation. The RF pulse was 50 kHz off-resonance, with a maximum field strength of 10 Gauss in the input object. The frequency encoding utilized an ADC dwelltime of 0.04 ms with 50 collected data points. A routine based on MATLAB function FSOLVE and Levenberg-Marquardt algorithm was used to reconstruct the 1D MR image profile at 50 spatial locations with the above Bloch-simulated signal.

**Results:** The signal expression (Eq. 1) was validated by the fact that the predicted MR signal perfectly matched with that obtained from Bloch simulation. The non-linear image reconstruction results are shown in Fig. 3, demonstrating that both magnitude  $|M_{\perp}|$  and the initial phase  $\phi_{init}$  profiles of the magnetization can be reconstructed using the proposed sequence and reconstruction. Note the presence of Gibbs-like ringing on the left side of the object, where acquired resolution is the lowest.

**Conclusions:** The theory for a Bloch-Siebert based RF frequency encoding method is presented with a proposed sequence design, signal expression derivation, and computer simulation as initial demonstrations. The method has the potential to achieve time-efficient RF-encoded acquisitions, without compromising flexibility in selecting image contrast.

**Reference:** [1] Hoult. JMR 1979; 33:183–197. [2] Canet. PNMR 1997; 30:101–135. [3] Sharp & King. MRM 2010; 63:151–161. [4] Katscher et al. MRM 2010; 63:1463–1470. [5] Kartäusch et al. ISMRM 2013; 0371. [6] Khalighi et al., MRM 2012; 68: 857–862.

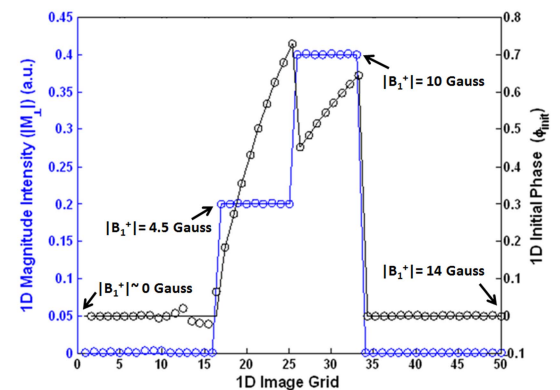


**Figure 3.** Non-linear image reconstruction demonstration based on Bloch-simulated MR signal. The true object is plotted with a solid line, and the reconstruction output is plotted with circles.